CSEM as a tool for better exploration decisions: Case studies from the Barents Sea, Norwegian Continental Shelf

Stein Fanavoll[1], Pål T. Gabrielsen[1], and Svein Ellingsrud[1]

Abstract

After more than 30 years of exploration and more than 100 wells drilled in the Barents Sea, only one field is in production and one is under development. However, recent discoveries made over the last three years have heightened the interest for exploration in the region. Nevertheless, the industry is still facing major challenges in finding commercial volumes of hydrocarbons, despite the fact that numerous wells have encountered shows or minor amounts of gas and oil, proving a working hydrocarbon system in large parts of the area. Since 2008, 3D controlled-source electromagnetic (CSEM) data have been acquired in the Barents Sea, providing additional geophysical information in the last three licensing rounds. In this paper, we showed how CSEM data can help the industry make better decisions in various stages of exploration. CSEM data, being sensitive to hydrocarbon saturation and volume, have the potential to reduce the risk of exploration failures of a prospect by influencing the chance of success and the expected size and volume. To illustrate this, we showed three case examples. (1) How CSEM can support certain play models, and hence, give valuable information in a license application phase as well as in drilling decisions. (2) How CSEM can support decisions to apply or not apply for certain blocks in a licensing round. (3) How CSEM can help prospect ranking and drill-or-drop decisions. All these three cases demonstrate the power of using CSEM as a complementary tool together with seismic data and other geologic information. This paper argues that CSEM data could have provided a correct prediction for all of the wells drilled in the Barents Sea where 3D CSEM data are available, provided there are sufficient sensitivity and 3D inversion results. This in turn proves the value of acquiring CSEM data in addition to seismic.

Introduction

Today, Norway is experiencing heightened interest for hydrocarbon exploration in the Barents Sea due to several recent discoveries. Skrugard and Havis (the future development area which is now referred to as "Johan Castberg") on the Polheim subplatform (Figure 1) are both substantial oil discoveries. The Norvarg gas discovery on the Bjarmeland platform in the northeastern Barents Sea, verified by well 7225/3-1, is opening up a large potential for the whole platform area, where exploration so far has encountered minor volumes only. However, the recent Wisting discovery has really made this part of the Barents Sea noteworthy due to significant quantities of light oil in a region where oil was not expected. Therefore, the Wisting discovery has not only raised the expectations for the surrounding areas, but also for the entire Barents Sea.

Exploration in the Barents Sea has not always produced success stories. Until now, over 100 exploration wells have been drilled on the Norwegian side, mainly during the 1980s and in the last decade. Most of these wells are either classified as dry, with shows only (breached seal), or as noncommercial discoveries. However, the wells verify the existence of a large working petroleum system across almost the entire Barents Sea. Nonetheless, after a period of more than 30 years of exploration, only one field is in production (Snohvit) and one undergoing development (Goliat). The four commercially viable, more recent discoveries (Skrugard, Norvarg, Havis, and Wisting), therefore, have revitalized the interest for the region as a hydrocarbon province. In addition, the Norwegian government has opened up 39,000 km^2 in the southeastern Barents Sea for hydrocarbon-related activities prior to the 23rd licensing round.

Historically, exploration wells in the Barents Sea have been drilled on the basis of seismic data, and usually on geologic structures only. Because EMGS began acquiring 3D controlled-source electromagnetic (CSEM) data in the Barents Sea in 2008, CSEM has been used as an interpretation tool combined with seismic (over 30,000 km^2 of multiclient data has been acquired during 2008, 2010, 2012, and 2013). Recent results show that combined interpretation can be powerful in the exploration phase (Darnet et al., 2007; Alcocer et al., 2012, 2013; Gabrielsen et al., 2013; Lorentz et al.,

[1]EMGS ASA, Trondheim, Norway. E-mail: sf@emgs.com; ptg@emgs.com; sve@emgs.com.

Manuscript received by the Editor 29 October 2013; revised manuscript received 6 February 2014; published online 20 May 2014. This paper appears in *Interpretation*, Vol. 2, No. 3 (August 2014); p. SH55–SH66, 10 FIGS., 1 TABLE.

http://dx.doi.org/10.1190/INT-2013-0171.1.

2013). CSEM data have been acquired over all the aforementioned, four recent discoveries, and the resistivity responses inverted from the CSEM data match well with the resource volumes that have been announced by the operators (Gabrielsen et al., 2013). CSEM has also been acquired over several other wells both before and after drilling, and the results are in accordance with the well data.

In this paper, we demonstrate how CSEM data can help oil companies improve their decisions throughout the exploration workflow regarding the definition of play models, where to apply for licenses, farming in–farming out, and prospect ranking within a production license. We also give a brief overview of the geology in the Barents Sea in light of the exploration history and new CSEM results. Finally, we present three case examples from different parts of the Barents Sea where CSEM may influence decisions.

Use of CSEM data in exploration

The electrical resistivity of the subsurface is a physical property that is strongly correlated with the fluid content and saturation of hydrocarbon reservoirs. The resistivity contrast between background geology and hydrocarbon reservoirs is often one or more orders of magnitude, making resistivity very suitable as a hydrocarbon indicator when measured from the seafloor (Eidesmo et al., 2002; Ellingsrud et al., 2002). The use of CSEM is also well described in a review paper by Constable (2010).

All multiclient CSEM data acquired in the Barents Sea are 3D wide-azimuth data. Staggered grids of receivers (all with multicomponent electric and magnetic sensors: Hx, Hy, Ex, and Ey) with 3-km receiver and line distance were acquired. The motivation for acquiring coarse grids was to improve operational speed and that the resolution is sufficient to detect most targets of interest in this early exploration phase. We do not have many direct comparisons with improved resolution from denser grids, except from the Polheim subplatform (case 3), where Nguyen et al. (2013) demonstrate improved resolution with a denser grid. With an average block size in the Barents Sea of 300 km^2, a typical receiver grid of approximately 120 receivers will cover three blocks at a time. With all receivers on the seafloor, the electric dipole source was towed close to the seafloor, transmitting a switched signal (Mittet and Schaug-Pettersen, 2008) with a frequency

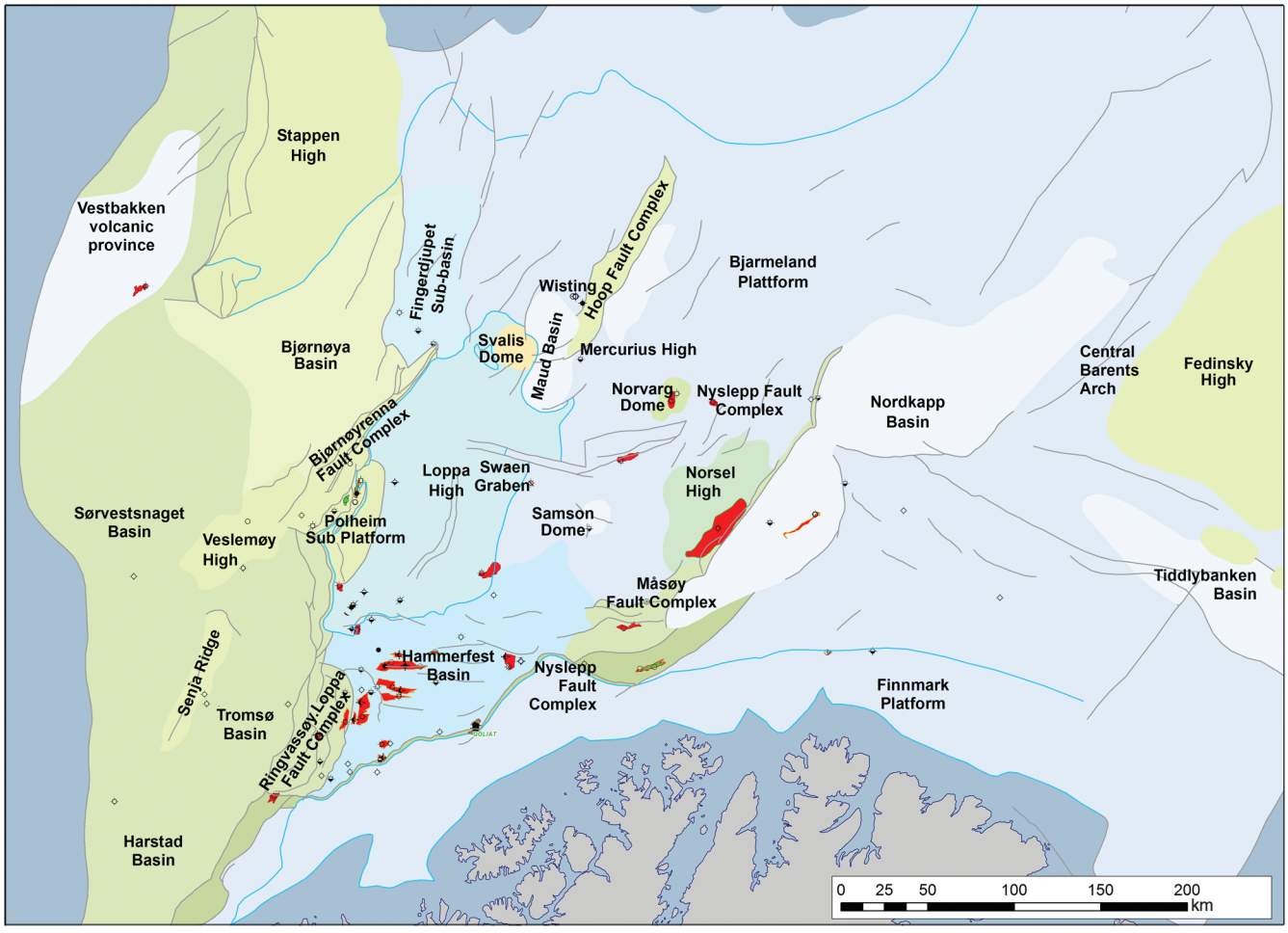

Figure 1. Overview of geologic provinces in the southern Norwegian Barents Sea.

content that is based on information from regional geology. A typical base frequency is between 0.2 and 1 Hz, with significant energy also on higher frequencies. Most receiver lines were towed in a north–south direction, and for some vintages also crosslines have been towed in east–west direction. Data are downloaded after retrieval of receivers, quality-checked, and preprocessed on the vessel.

In the following case examples, the CSEM data are inverted into 3D earth resistivity models. The inversion uses a 3D finite-difference time-domain modeling code and a Broyden-Fletcher-Goldfarb-Shanno algorithm for the model update (Maaø, 2007; Zach et al., 2008; Mittet, 2010). The inversion assumes the earth to be transversely isotropic with a vertical axis of symmetry (VTI media). This provides an earth model for the horizontal and vertical resistivity. All cases shown are obtained from unconstrained inversions, which mean that the inversion is purely CSEM data driven with no external input besides the inversion start model. The start models are constructed based on lower dimension inversions (1D and 2.5D) together with regional depth surfaces such as the seabed and the Base Cretaceous unconformity. For most of the cases, the 3D inversion models are run with a cell size of 200 m in the x- and y-directions and 50 m in the z-direction. Inline and azimuthal receivers are input to the inversion ensuring optimal illumination of the earth as well as inline and broadside information. All inversions are using electrical sensor data (Ex and Ey) where a signal and estimated noise are used. The receiver data can therefore be weighted according to the signal-to-noise ratio. Typical background noise levels for the electrical sensor data are from 1×10^{-11} to 1×10^{-10} V/m. Occasional noise bursts due to large solar activity may occur and increase the noise level with as much as one to two decades. Different frequency contents for the inversion have been used for the different cases depending on the acquisition source parameters; but in general, frequencies are in the range of 0.2–3.0 Hz. Source-receiver offsets used are in the range of 1–10 km. The inversion results discussed in this paper are taken from an iteration after the inversion has converged. Generally, the total inversion data misfit at convergence ranges from 1.0 to 1.5 times the data uncertainty.

The end results from 3D inversion are earth model cubes of horizontal and vertical resistivity, displayed by using a color scale where red represents high resistivity and blue/purple low resistivity. A thin resistor is only imaged by the vertical resistivity component and not the horizontal resistivity component. This is a result of fundamental difference to the CSEM data sensitivity and not necessarily a property of the resistive layer itself (e.g., if compared to a resistivity log). A consequence is that the anisotropy factor, calculated by dividing the vertical by the horizontal resistivity, will exhibit with an anomalously high (apparent) anisotropy for a thin horizontal resistor (e.g., a hydrocarbon-filled reservoir). In other words, the anisotropy factor can be used as a "thin, resistive-layer indicator." Therefore, handling and understanding anisotropy are important aspects of a CSEM interpretation workflow (Ellis and Newton, 2013; Narongsirikul et al., 2013). An example of this is shown by the map of the Barents Sea in Figure 2, where the apparent anisotropy is overlaid to some blocks where CSEM data were acquired, giving a regional view of the resistivity. In addition, resistivity maps can provide valuable information on the lateral extent of a charged reservoir. Combining the lateral extent with the resistivity thickness product also obtained by inversion, CSEM data can be used to estimate volumes (Baltar and Roth, 2013).

As mentioned, the extensive coverage with CSEM data not only gives a regional overview of the resistivity distribution but also maps out resistivity anomalies, or thin resistors that could identify hydrocarbon-filled traps. CSEM is sensitive to all kinds of thin resistors, also to charged stratigraphic traps and lithologies with higher resistivity than the surrounding geology. CSEM data can therefore give a new and improved picture of the geology in the Barents Sea and support better decisions in the exploration phase regarding farming in–farming out of blocks, well positioning, and provide justification for new play types, and potentially improve the understanding of the prospectivity in the entire region.

Other lithology, deposition environments, or structures not associated with hydrocarbons that may cause resistive anomalies are volcanic provinces, salt basins and salt diapirs, basement highs, and carbonate platforms, which all must be considered when interpreting CSEM data. These rock types are highly resistive and will influence CSEM measurements. Thorough understanding of the geology is therefore imperative to interpret the CSEM data correctly.

CSEM results are of little value unless they are interpreted in conjunction with other geophysical and geologic information such as seismic and well data. Furthermore, interpretation of CSEM data must be incorporated in the company's risking procedure, similar to incorporation of other geophysical data, to handle the associated uncertainties and probabilities. This will, in conjunction with volume estimates, form a basis for improved decisions in exploration.

Barents Sea overview — Geologic history and prospectivity in light of CSEM results

The Barents Sea covers a vast area (~200,000 km^2 in the southern, Norwegian part), and despite more than 30 years of drilling history, large parts are unexplored (Figure 1). Most of the wells are concentrated in the southwest, in the Hammerfest Basin, the Loppa High, and the Polheim subplatform. The geology is highly variable, ranging from Tertiary Basins in the west, Jurassic Basins (e.g., Hammerfest Basin) in the middle part, and Triassic and Permian platforms (e.g., Bjarmeland Platform and Finnmark Platform, respectively) in the east.

If we look apart from the reasonable drilling success of the last three years, there are still major uncertainties regarding the prospectivity of some areas in the Norwegian Barents Sea. To a large extent, this is related to models for reservoir rocks, especially in the Cretaceous and the Triassic, where several possible play models are not confirmed by earlier drilling. It therefore seems reasonable that new ideas are needed to increase the future success rate in the Barents Sea.

From 2008 to 2013, EMGS has built up a substantial EM multiclient library, as shown in Figure 2. If we look at the survey results processed so far, we see that these data indicate a substantial potential for additional resources in different parts of the Barents Sea. In the multiclient campaigns, approximately 20 well locations were covered by 3D CSEM. Some were drilled prior to acquisition, thus acting as calibration, and some have been drilled after acquisition. Out of these locations, only three may be considered as showing inconclusive CSEM results, mainly due to the lack of sensitivity to the target or to the fact that no full 3D inversion has been carried out. In short, we conclude that all significant discoveries are clearly imaged by the CSEM data whereas noncommercial or dry wells all exhibit a lack of CSEM response.

The apparent anisotropy map in Figure 2 shows numerous resistive anomalies that have not yet been drilled. The crucial question is then: What do all these undrilled anomalies represent? Of course, there is no one answer to this question. Factors such as the structural and stratigraphic setting play a role in assessing a CSEM anomaly. Some of these anomalies conform to structure; others require a stratigraphic closure to define a prospect. The stratigraphic setting varies from Triassic to Tertiary, and the background resistivities vary from 1 to 100 Ωm (Fanavoll et al., 2012). All these factors must be carefully assessed in an integrated interpretation procedure. What one could say at an early stage is that it seems unlikely that all anomalies represent hydrocarbon accumulations. On the other hand, it is equally unlikely that none of them represent hydrocarbon accumulations, and the enormous potential these anomalies represent justifies not only a fully integrated geophysical approach including available geophysical and geologic data, but also drilling to test some of the scenarios.

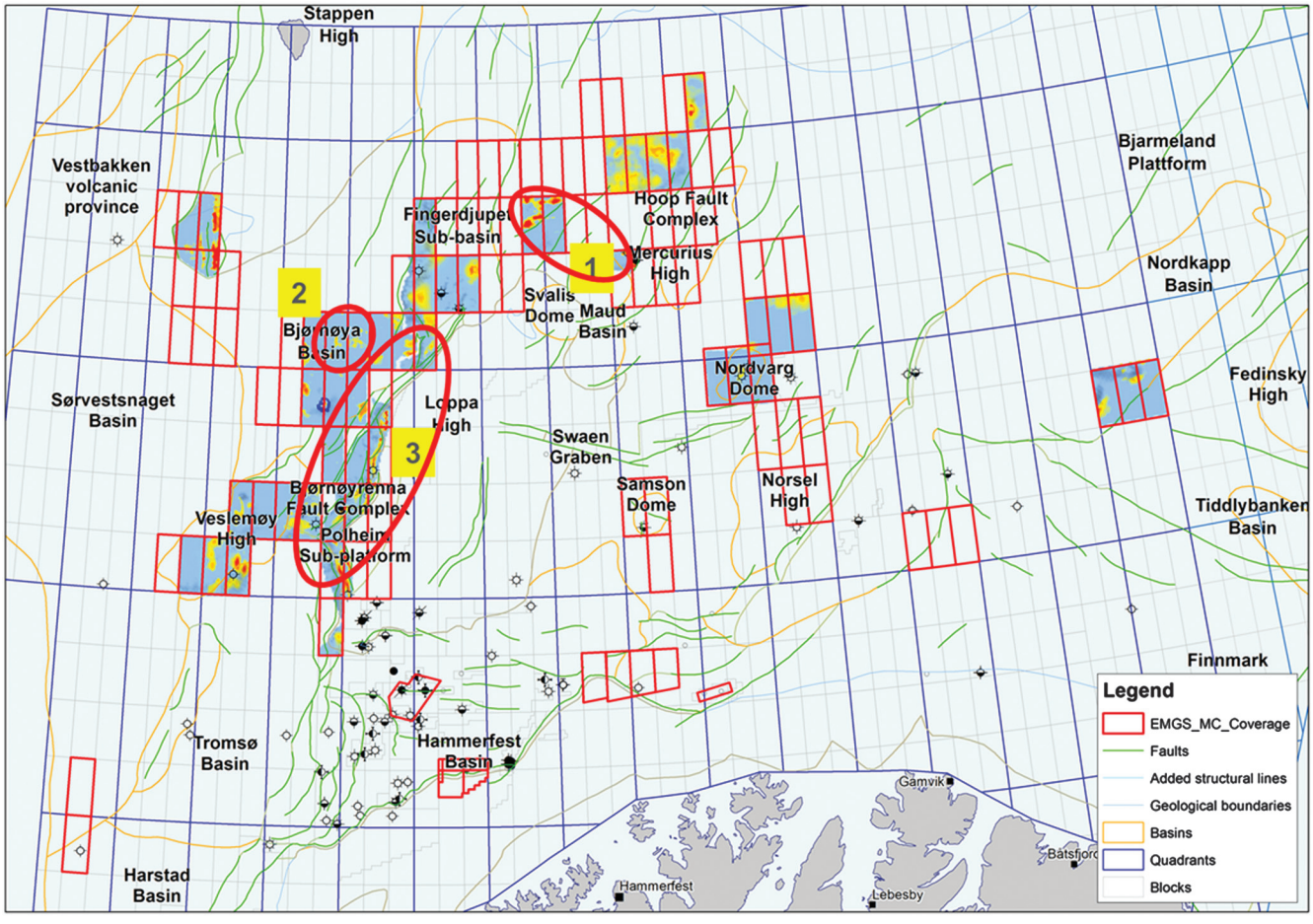

Figure 2. Overview of multiclient EM acquisition in the Barents Sea (red rectangles: acquired blocks, black rectangles: planned acquisition). Also shown are selected inversion results (apparent anisotropy) in selected blocks where multiclient data have been acquired. The location of the three case examples are shown with numbers 1–3.

Below, we show three case examples focusing on different aspects of the exploration workflow. These examples are labeled 1 to 3 in Figure 2.

Case studies

The hoop area — Different play models

In the last three licensing rounds in the Barents Sea, much emphasis has been placed on the northern part of the structural element called *the Bjarmeland Platform*. A total of 15 blocks have been awarded in an area commonly referred to as "Hoop" (from the Hoop Fault Complex, a dominating structural element in the area (label "1" in Figure 2) and substantial volumes of 3D seismic and 3D CSEM have been acquired, also in 2013 (Figure 2). Earlier exploration on the Bjarmeland platform has been concentrated further south of Hoop, but until the gas discovery of Norvarg was announced in 2011, no significant discoveries were made. However, except for a few wells, all wells exhibit shows or minor amounts of hydrocarbons, demonstrating that there is indeed a working hydrocarbon system in the area. One of the targets in south of Hoop has been in the Triassic succession, but the main problem has been lack of high-quality reservoir sands and sufficient volumes. In this case example, we illustrate how a new play model can be upgraded based on the integration of CSEM and seismic.

On 6 September 2013, the Austrian oil company OMV announced an oil discovery in license PL537 on the Wisting prospect in Lower- to Middle Jurassic reservoir rocks. An oil column of 50–60 m was reported with potentially recoverable reserves of 60–130 MMboe. The discovery was associated with a significant EM anomaly (Figure 3) as well as a seismic AVO response. Located at a very shallow depth (~300 m bml), CSEM would be sensitive to almost any accumulation provided the existence of a sufficient resistivity contrast. On this location, there is a high degree of correlation between the seismic and CSEM results. The CSEM anomaly seems to conform to structure and matches well in depth and lateral extent with the seismic amplitude anomaly. One should keep this in mind when planning for other wells targeting similar prospects in the area.

The most important result of the Wisting discovery from a commercial- and CSEM perspective is probably the fact that it was an (light) oil. Due to the highly resistive background in the area, it has been argued that hydrocarbons, and in particular oil, cannot be seen. The Wisting well shows that this is not the case, and we believe that these results will have implications for future exploration in the Hoop area. In the same license, a second well that targeted a deeper stratigraphic level was subsequently drilled, deliberately avoiding any shallow CSEM anomaly. However, this well was dry. This is in accordance with the CSEM results, also when taking into account the reduced sensitivity to the deeper target.

The Wisting discovery opens up for additional oil discoveries in the area, and the CSEM data reveal large anomalies that should be subject to further investigation.

Judging from the lack of exploration success on the Bjarmeland platform, and in particular the problem related to the lack of a high-quality reservoir sands in the Triassic succession, it is obvious that new ideas and methods for detection of hydrocarbons should be tested to increase exploration success. Recently, ideas have been launched that argue for a different depositional environment in the upper Triassic that may give rise to larger volumes and better reservoir development (Kjølhamar, 2012). This idea is supported by the inversion results from the CSEM data, where we see CSEM anomalies in the area where these Triassic reservoirs are assumed to be present (Fanavoll et al., 2013).

How should these anomalies be interpreted? By studying the map for two of the blocks in the area (Figure 4), we immediately see that there is little correlation between the shallow Jurassic structure and CSEM anomalies. This suggests that if the anomalies are caused by hydrocarbons, the traps will partly need stratigraphic closure and/or fault seal. Also, these resistive anomalies seem to represent a deeper source for resistivity than the Wisting discovery. Furthermore, the structural closure in the south should be associated with high risk because there is no resistive anomaly associated with the structure. If one believes it is filled with hydrocarbons, the reservoir resistivity has to be much lower than for Wisting given the structure's low-resistivity measurement, which differs significantly from what was measured on Wisting.

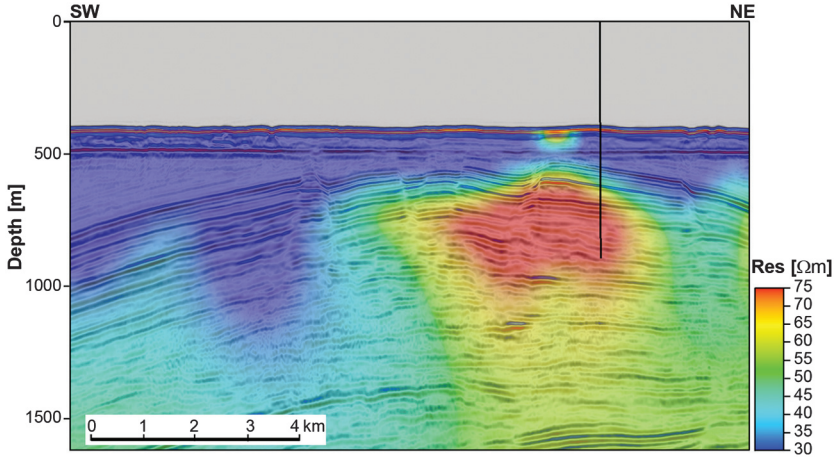

Figure 3. The Wisting oil discovery as imaged by 3D CSEM inversion (vertical resistivity), displayed on a seismic line. The black line indicates the well location. The CSEM results clearly indicate presence of hydrocarbons in two fault blocks in the northeastern part of the larger structure whereas the southwestern part seems to be dry.

It is clear that exploration in these two blocks raises a fundamental question: Which play model should be pursued: the resistive Triassic target or the relatively conductive Jurassic target? Making the right decisions will be of enormous value to the industry, especially because the same question also applies for many of the other licenses in the entire Hoop area.

To build a viable geologic model that can explain the CSEM results, a fully integrated approach including seismic AVO and inversion, well results, and other geologic information is needed. The four most important aspects in this workflow are as follows:

1) Burial and uplift history: Will reservoir porosity be preserved after being buried as much as 2 km deeper than today?
2) Seismic expression: Looking for geometries that can explain the CSEM results may be a challenge (Figure 5), but careful and focused reprocessing could improve the image considerably. Seismic AVO analysis and inversion for porosity will also guide the assessment of different geologic models, although a challenge is that no nearby wells are available.
3) High-resistive background: How does a hydrocarbon reservoir behave in a highly resistive background? Typical reservoirs in other regions (e.g., the North Sea) show resistivity values in the range of what we see in the background of the Hoop area. However, recent wells indicate that it is likely to expect much higher resistivities provided there is a high-quality reservoir (e.g., the Jurassic reservoir in Norvarg is known to have more than several hundred Ωm). The log values on Wisting are not known to date, but comparison of the inversion results indicates significantly higher values.
4) Risking and expected value: using CSEM in the risking procedure for the calculation of the probability of success (POS) in combination with volume estimates will guide the explorationists in their decisions. With the limited well control available today the targets are considered as high-risk but also very high-reward targets.

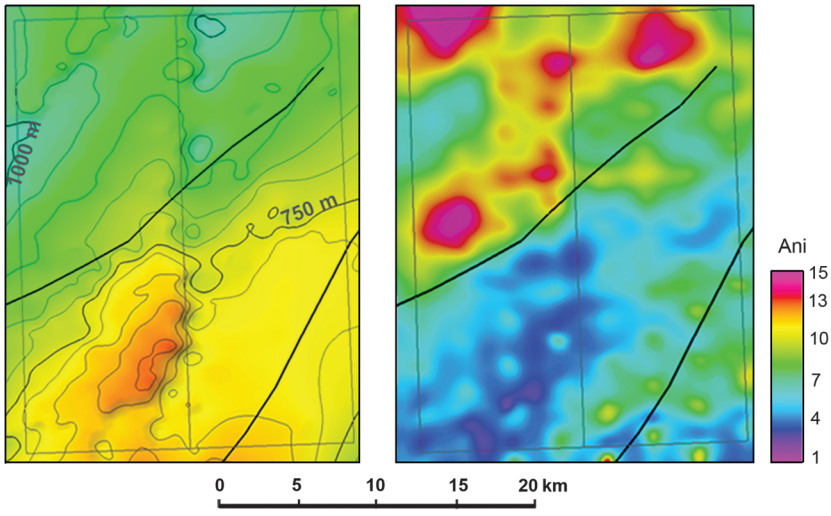

Figure 4. Structure map and CSEM results from two blocks northwest of the Wisting discovery. The depth structure map of Base Cretaceous unconformity (left) indicates a large, shallow structural closure (contour interval 50 m), whereas the CSEM anisotropy anomaly map (right) shows resistive anomalies in the northern part, which to some extent need a stratigraphic trapping element if they are associated with hydrocarbon accumulation. There is no resistive anomaly associated with the structure.

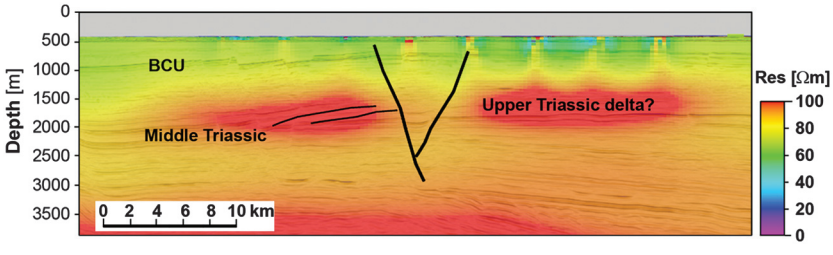

Figure 5. Seismic profile overlaid by 3D CSEM inversion result (vertical resistivity). To some extent, there is a correlation with fault pattern, and the anomalies are associated with a possible prograding delta system interval in the Upper Triassic. The burial depth to a possible target is 1200–1300 m.

In conclusion, we see that CSEM data have the potential of providing valuable information for future exploration in the Hoop area. The enormous potential indicated by the CSEM anomalies certainly justifies a profound assessment and even consecutive drilling.

Bjørnøya Basin — Integrated approach for fluid contact interpretation and resource estimation

An important aspect of prospect evaluation is to consider the POS and calculate the expected volume of resources. This is important information to have before a license application and at a later stage before a drill-drop decision. This second case example will demonstrate how the integration of seismic and CSEM data can impact the probability of geologic success and the estimation of expected resources for a particular prospect in the Bjørnøya Basin.

Within the Bjørnøya Basin in the western Barents Sea, a distinct shallow seismic amplitude anomaly can be observed close to the Base Tertiary horizon. The seismic amplitude exhibits a soft response indicating that it may represent presence of gas. By comparing the seismic section and the CSEM anomaly, we see that the resistivity

anomaly coincides with the thicker updip part of the seismic amplitudes whereas the thinner part exhibits no CSEM anomaly. It is well known that seismic data are also sensitive to the presence of very low saturation gas (fizz gas) whereas CSEM is more sensitive to high hydrocarbon saturation in sediments (usually > 60%) (Constable, 2010). The lack of CSEM response could therefore be explained by low saturation gas in the thinner section.

Alternatively, the difference in the seismic and CSEM responses in the thin section could be caused by the fact that this part of the reservoir was too thin to be detected by CSEM. An extensive CSEM modeling and inversion study was therefore carried out to investigate the CSEM sensitivity to the seismic-defined prospect. The modeling study used the same receiver layout as in the real survey. Three different, anisotropic earth models were used, representing the reservoir filled to a minimum, medium, and maximum extent based on mapped outlines from seismic data (Figure 6). The inverted results from the synthetic data indeed show that the CSEM measurement is sensitive to the total lateral extent of the reservoir, also including the thinner part. The results also show a strong correlation with the reservoir thickness variations, as expected.

The results suggest that it is useful and important to combine the CSEM and seismic data to argue for the presence of a new and more likely prospect outline. The integrated approach is shown in Figure 7. Figure 7b shows that the CSEM anomaly from the real data covers an even smaller part than the minimum case based on interpreting the seismic data only. Therefore, a new outline defined by the CSEM anomaly can suggest a new fluid contact to define the prospect. This is exemplified in Figure 7c where the top reservoir horizon is cut at a new interpreted fluid contact at 910 m. Note that the outlines defined by the top reservoir seismic horizon (Figure 7c) and the CSEM anomaly (Figure 7b) are very similar. The CSEM anomaly correlates almost perfectly with the northern part of the prospect structure, and the integrated interpretation indicates that the gas–water contact (GWC) is higher (20–25 m) than anticipated from the seismic data. It is an interesting observation that the fairly thick part of the seismic prospect in the southwest, which would have given a strong CSEM anomaly according to the modeling study (Figure 6), is significantly smaller using the new GWC at 910 m in Figure 7c. Furthermore, a weak resistive anomaly (Figure 7b) indicates that the two segments, although possibly not in communication, share a common GWC. Such a correlation between seismic and CSEM results increases the POS for the prospect, but at the same time decreases the expected size of the target thus reducing the expected volume of hydrocarbon resources.

The expected resources in the prospect can be estimated by using CSEM data and the seismic data separately. The resources estimated from CSEM data use the volume calculation methodology described by Baltar and Roth (2013). The method uses a Monte Carlo simulation for estimation of a net pay volume probability distribution from the CSEM inversion result (see

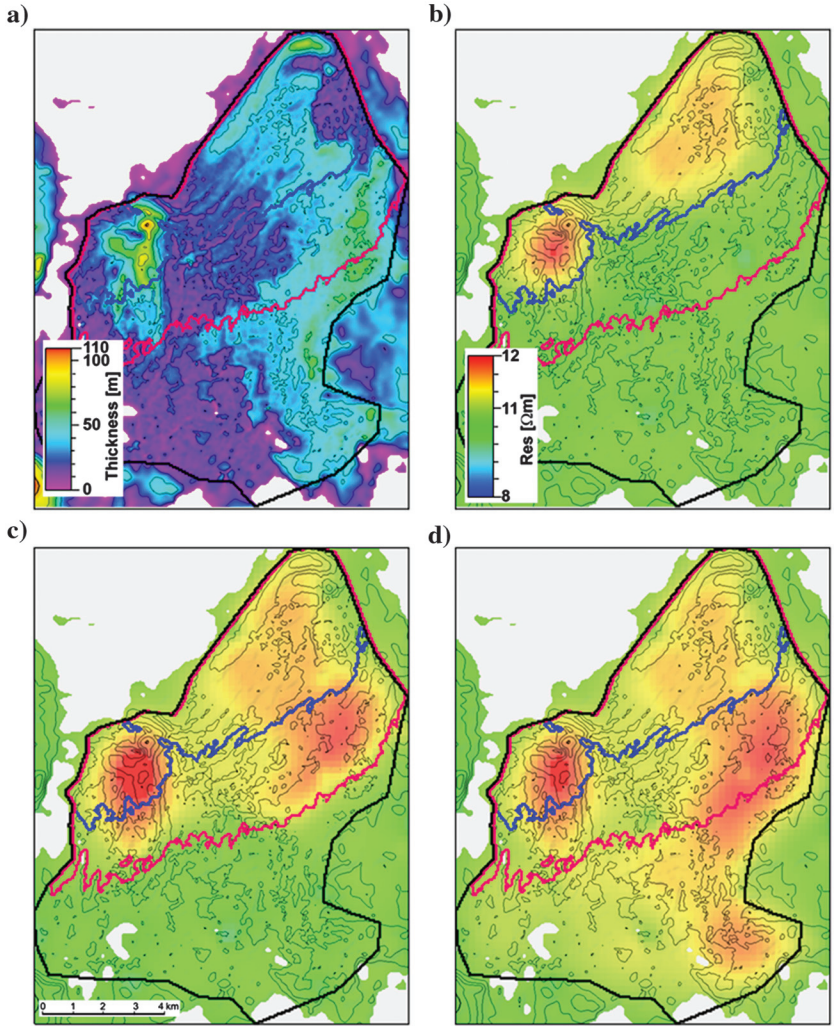

Figure 6. The 3D inversion of synthetic CSEM data shows that lateral extent of the prospect can be interpreted on average resistivity maps (average resistivity is calculated in a certain interval relative to the Base Tertiary horizon). The resistivity response is also clearly linked to the reservoir thickness variations. (a) Reservoir thickness map. (b) Average resistivity map of a minimum prospect scenario (blue polygon). (c) Average resistivity map of a medium prospect scenario (red polygon). (d) Average resistivity map of a maximum prospect scenario (black polygon). Courtesy: Det Norske.

Figure 7b). The method relies on the sensitivity of CSEM data to the net volume of resistive rock and on the transverse resistance equivalence principle to relate the low-resolution inversion result to possible reservoir scenarios at the well log scale. We can also estimate the rock volume based on the seismic data using our new integrated prospect outline (Figure 7c), and calculate the thickness between the top reservoir horizon and a fluid contact at 910 m. We anticipate the estimated seismic rock volume to be at the high end of the calculated CSEM rock volume. This is because the seismic rock volume based on the thickness maps assumes that reservoir sand exists all the way from top reservoir to the fluid contact (gross rock volume) whereas the CSEM methodology calculates the net pay volume. Figure 8 shows the CSEM rock volume probability curve and the calculated seismic rock volume. Because the seismic rock volume is at the 95th percentile of the CSEM rock volume, the results suggest that the net sand thickness is much less than the maximum possible reservoir thickness inferred from the seismic data. From the Monte Carlo simulation of the CSEM data, a net thickness distribution between 5 and 40 m is calculated with a mean average of 18-m net pay. This assumes a normal reservoir net resistivity between 150 and 1000 Ωm (from well logs), corresponding to a hydrocarbon saturation between 75% and 90% using Archie's formula. From the CSEM net rock volume curve in Figure 8 and parameters given in Table 1, the mean recoverable resources are estimated to be 75 MMboe for this particular prospect. This is considerably smaller than the maximum scenario mapped by the extent of the seismic amplitude anomaly (Figure 7). Keeping this in mind, for instance during a license application stage, it is obvious that such knowledge is of value when a decision whether to apply for a specific block or not is about to be taken.

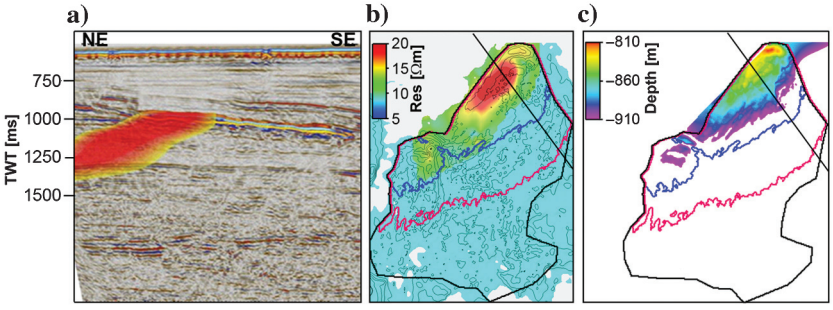

Figure 7. (a) A shallow prospect is defined by a soft seismic response. Together with the seismic section is a horizon slice of the CSEM anomaly. The resistive anomaly is only present in the updip part of the prospect. (b) Average resistivity map from CSEM inversion displayed with contoured reservoir thickness. Minimum (blue), medium (red), and maximum (black) scenarios based on seismic data are given by the three polygons. The resistive anomaly suggests that the prospect extent is smaller than the minimum prospect outline. (c) Top reservoir horizon cut at an interpreted fluid contact at 910 m. Note the resemblance of the prospect extent with the resistive anomaly in (b). The black solid line in (b) and c) shows the position of the seismic line in (a). Courtesy: Det Norske.

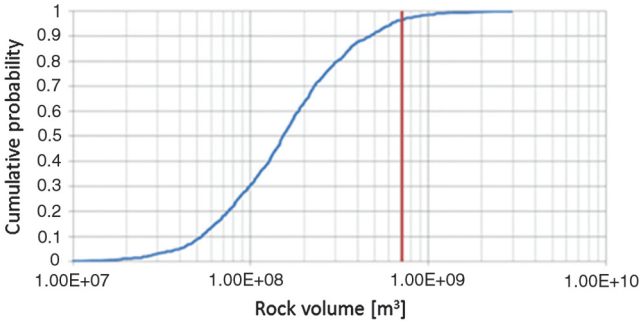

Figure 8. Rock volume calculation of the prospect based on CSEM data (blue line) and seismic data using new interpreted fluid contact from Figure 7c. The seismic rock volume is at the upper percentile of the CSEM curve. This is expected because the CSEM provides net rock volume whereas the seismic data give gross rock volume.

Table 1. Parameters used to calculate recoverable resources.

Average water saturation	18%
Average porosity	20%
Formation volume factor	1.2
Recovery factor	40%

Polheim subplatform and Bjørnøyrenna Fault Complex — Looking for analogs

Case example three will show how drilled targets (commercial and noncommercial) are correctly predicted by CSEM data. Besides the fact that the predictions themselves for most of these wells could have been used to optimize the success rate, they can now be used as CSEM calibration points and analogs for further interpretation of the Polheim subplatform and the Bjørnøyrenna Fault Complex (Figure 1). This information should ideally influence decisions regarding future drilling and maturing of leads and prospects. The data examples from this area calibrate CSEM data with well results and identify several new leads based on combined CSEM and seismic interpretation.

The Polheim subplatform and the Bjørnøyrenna Fault Complex separate the Loppa high to the east from the Bjørnøya Basin to the west. Skrugard and Havis were discovered on the Polheim subplatform in 2011 and 2012. The Skrugard discovery is reported to have a double flat spot on the seismic data (gas–oil and oil–water contacts) and the Havis discovery one flat spot (published in presentations by Statoil). The two

oil and gas discoveries boosted the interest in the Barents Sea because they proved oil in the Middle to Lower Jurassic play.

In 1987, well 7219/9-1 was drilled for the same play types only a few kilometers southwest of what is now the Johan Castberg discovery (Havis and Skrugard). This well encountered excellent reservoir quality in the Lower to Middle Jurassic, but only with shows. The Nunatak well (7220/5-2 drilled in 2013) located north of Skrugard was drilled to test a play in the Lower Cretaceous. Parts of the prospect outline overlapped the Skrugard discovery. The well was considered high risk, and only noncommercial gas in poor reservoir quality was found. Further south on the Polheim subplatform, another well targeted the plays in Lower Cretaceous and Lower to Middle Jurassic (the Salina well 7220/10-1 drilled in 2012). This well only exhibited small amounts of gas and condensate at both target levels.

It has previously been demonstrated (Gabrielsen et al., 2013; Nguyen et al., 2013) that Skrugard and Havis are identified with CSEM data because resistive anomalies and that no resistive anomaly is found at the location of dry well 7219/9-1. Furthermore, Figure 9 shows that the noncommercial Salina and Nunatak wells are not associated with any significant resistive anomaly. However, the Nunatak well is located just at the southern edge of a large CSEM anomaly and should therefore be associated with more uncertainty than the Salina well that is located some distance away from the nearest resistive anomaly. In total, Figure 9 shows six wells where CSEM provided a correct prediction for the Lower to Middle Jurassic and Lower Cretaceous plays along the Bjørnøyrenna Fault Complex. Three of the wells are significant discoveries (Havis 7220/7-1, Skrugard 7220/8-1, and 7220/5-1) and three wells are noncommercial or dry (7219/9-1, Salina 7220/10-1, and Nunatak 7220/5-2). This demonstrates that CSEM data are able to separate commercial hydrocarbon-bearing reservoirs from nonhydrocarbon reservoirs in this area. The last well that was drilled (Skavl) also revealed oil and gas as predicted by CSEM, and although being a rather small discovery, it will provide valuable additional reserves to the development of Johan Castberg.

Although Johan Castberg has confirmed an oil play in this part of the Barents Sea, there is still a great risk in basing drilling decisions on seismic-defined structures and AVO responses only (e.g., the Salina well and 7219/9-1). The main play risk is associated with Cenozoic uplift and erosion. This can cause expansion of gas resulting in the spilling of earlier trapped oil and reduced overburden, leading to reactivation of faults and breaching of seals. This in turn can have the effect that perfect looking reservoirs on seismic with structural closure and AVO responses are in fact blown traps with only low hydrocarbon saturation. In addition, the Upper Jurassic–Lower Cretaceous play involves high risk with respect to reservoir presence and reservoir quality. Combining seismic data with CSEM data is therefore a large risk reducer because a resistive anomaly associated with a seismic-defined structure or AVO response can separate high-hydrocarbon-saturated reservoirs from low-hydrocarbon-saturated reservoirs. The main pitfall with a resistive anomaly in this area is probably mature source rock in the Upper Jurassic and possibly the Cretaceous that show high resistivity (20–40 Ω m) from other wells (e.g., well 7219/8-1). In addition, a well further north in the Fingerdjupet area (7321/7-1) penetrates what we interpret to be cemented sandstone with high resistivity (60 Ωm). However, these resistive anomalies are much lower than what is shown from the Skrugard well that has a peak value above 1000 Ωm (Løseth et al., 2013).

Figure 10 shows three leads on the Polheim subplatform and along the Bjørnøyrenna Fault Complex where multiclient 3D CSEM and 2D seismic data are integrated. Two of the leads are interpreted to be analogs with the Lower to Middle Jurassic reservoirs penetrated by the wells discussed earlier (Figure 10a and 10b). For confidentiality reasons, the location of these leads will remain unknown to the reader. The third lead

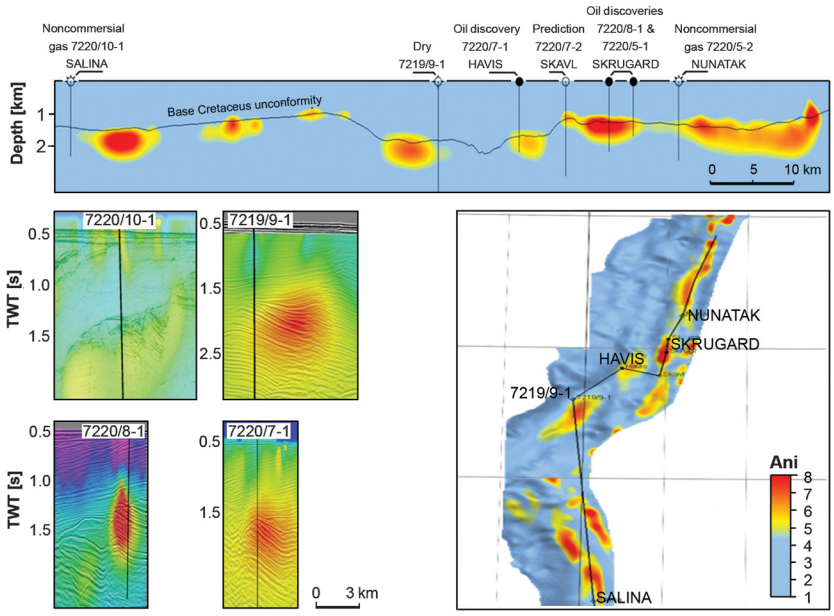

Figure 9. (a) Apparent anisotropy section along the Polheim platform from the Salina well in the south to Nunatak in the north. (b) Seismic sections with CSEM data (vertical resistivity) overlaid through some of the wells. (c) Apparent anisotropy map with the cross-section track and well positions. The examples illustrate that CSEM is able to separate the noncommercial discoveries from the commercial discoveries on the Polheim platform.

is located east of well 7219/9-1 (Figures 9 and 10c) and is interpreted to be associated with the Lower Cretaceous–Upper Jurassic section. The different leads show integration of seismic data with three different CSEM attributes.

Through a cooperation between multiclient geophysical (MCG) and EMGS, seismic and CSEM data have been interpreted and integrated (Figure 10a). An interpretation of the deltaic Lower to Middle Jurassic sand is shown in yellow and Lower Cretaceous fans are shown in green. Structural closure is identified for the deltaic sand whereas the Lower Cretaceous fans need a combined structural-stratigraphic trap. CSEM data (anomalous vertical resistivity) overlay the seismic data to the right in Figure 10a. This CSEM attribute emphasizes anomalous resistivity values and is calculated by subtracting a background resistivity model from the vertical resistivity model obtained from inversion (Gabrielsen et al., 2013). A value close to zero is interpreted to be part of the background resistivity trend whereas higher values indicate thin resistors. Two anomalous resistors are observed (lead Eivind and Eivind2 U.), which can be linked to the Lower to Middle Jurassic and Lower Cretaceous reservoirs, respectively.

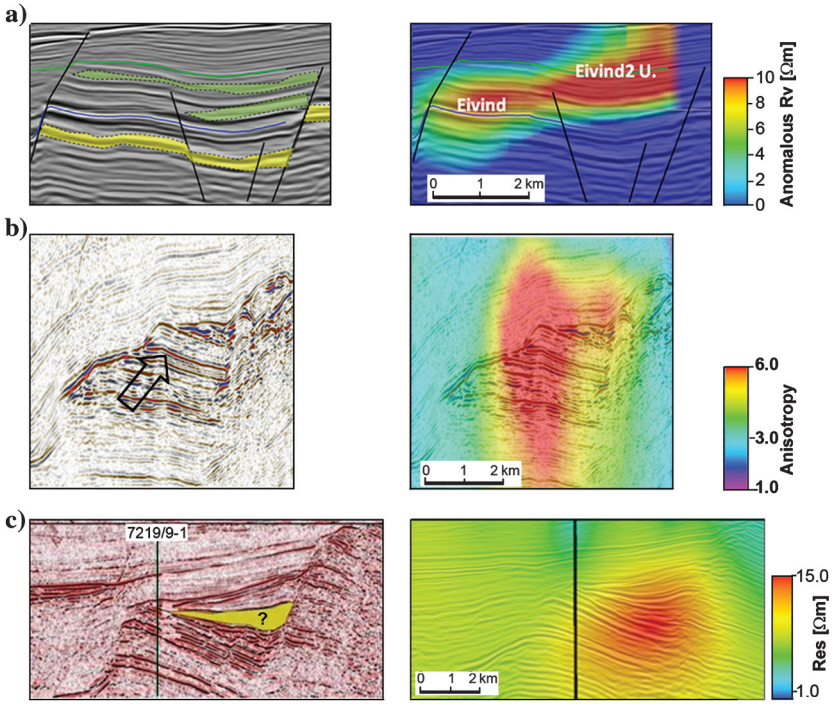

Figure 10. Three leads based on seismic and CSEM data along the Bjørnøyrenna Fault Complex. (a) To the left: Possible Lower Cretaceous fans (green) and Lower to Middle Jurassic deltaic sand (yellow). To the right: The CSEM attribute anomalous vertical resistivity (ARv) increases probability of hydrocarbon accumulation in both plays (seismic data and sand interpretation from MCG) (b) Possible flat spot identified in Lower to Middle Jurassic sandstone (left) that is also associated with a CSEM apparent anisotropy anomaly (right) (public seismic data). (c) To the left is prediction of sand interval (by FugroJason) in syn-rift Lower Cretaceous sediments (Carstens, 2009) and seismic overlaid by CSEM resistivity (Rv) to the right (seismic courtesy of MCG). Target depths are in the range of 1200–1600 m below mud line.

In Figure 10b, a possible flat spot is identified on 2D seismic data in a rotated fault block. The flat spot is interpreted to be in the Middle Jurassic. The CSEM attribute apparent anisotropy overlays the seismic data to the right. Apparent anisotropy is calculated by dividing the inverted vertical resistivity model by the horizontal resistivity model. This attribute emphasizes thin resistors because thin resistors are only imaged in the vertical resistivity model and not in the horizontal resistivity model in an unconstrained inversion (Alcocer et al., 2013; Gabrielsen et al., 2013). The apparent anisotropy shows an anomaly located in the same position as the flat spot on the seismic.

The last example is within Upper Jurassic to Lower Cretaceous syn-rift sediments southeast of the dry well 7219/9-1 (Figures 9 and 10c). Sand is predicted to be present in the syn-rift sediments by seismic inversion (Figure 10c left) by Fugro Jason in 2009 (Carstens, 2009) and also by interpreting seismic stratigraphy and facies (Gerdes et al., 1992; Gabrielsen, 1994). A vertical resistivity anomaly is identified to be located in these syn-rift sediments (Figures 9 and 10c right). The depth of this resistive anomaly is uncertain. For example, Nguyen et al. (2013) use an exclusive CSEM data set with a denser receiver grid covering the same anomaly. This improves the vertical resolution of the inversion image and also moves the resistive anomaly toward the upper part of the syn-rift section.

The two first leads in Figure 10 show resistive anomalies in Lower to Middle Jurassic sands located in a rotated fault block. One of them also shows indications of a flat spot on the 2D seismic data. These leads are interesting because they can be regarded as analogs to the Havis and Skrugard discoveries. For example, the Skrugard discovery well 7220/8-1 (Figure 9b) shows a very similar CSEM expression as the lead in Figure 10b. The leads in the Upper Jurassic to Lower Cretaceous syn-rift sediments (Figure 10a [Eivind 2U] and 10c) are different because they represent a different play model that to date is not proven to be of commercial value in the area. This play is associated with high risk based on reservoir presence and quality, and a hydrocarbon trap would require a combined structural and stratigraphic element. Several other explanations have been posed to explain this anomaly, such as mature source rock in the Upper Jurassic. The strongest argument against the latter model is that the source rock resistivity is not proven

to be high enough to create the strong resistive anomaly observed.

Conclusion

The history of exploration in the Barents Sea cannot be regarded as very successful, despite recent discoveries. However, there are ideas for new play models that have not yet been explored, and there are large unexplored areas (in the range of 100,000 km^2) in this vast and remote offshore area.

With successive data acquisition campaigns since 2008, entire regions are now covered by 3D CSEM data. The availability of data opens up for new geologic interpretations in addition to specific prospect mapping. This can offer valuable help in an early stage of exploration. The coverage of 3D multiclient CSEM data allows for calibration with more than 20 wells, some drilled before and some after CSEM acquisition. We argue that for all these wells, CSEM accurately predicts the outcome of drilling, both for the dry cases, the minor discoveries, and the significant discoveries. This knowledge can in turn be used to better derisk new prospects.

For screening purposes, the use of a CSEM anomaly map can make exploration more efficient by limiting the area of interest and focusing interpretation within the anomalous area. In a license application phase, this will aid the explorationist in making better decisions. In all cases, it is imperative that CSEM data should be interpreted in an integrated fashion with other geophysical and geologic information.

Judging from what appears to be a convincing track record for CSEM in the Barents Sea, CSEM data have the potential to influence exploration decisions to a larger extent than to date, not only decisions on where to drill, but also where not to drill. Seeing that all the significant discoveries in the Barents Sea to date are associated with resistive anomalies, one needs very convincing arguments if one wants to drill in a location where there is no resistive response, e.g., where prospects are too deep to be detected by CSEM.

By acknowledging the value of the CSEM results, the petroleum industry can use them in various stages of exploration, such as license application work, prospect ranking, drill-drop decisions, and farm-in–farm-out decisions.

Acknowledgments

The authors thank EMGS for permission to publish this article. Furthermore, we would like to thank Det Norske Oil Company for permission to use the results from a modeling and inversion study carried out in the Bjørnøya Basin. Some examples are also taken from the joint project between EMGS and multiclient geophysical for seismic and CSEM integration. We also thank our colleagues V. Furuholt for creating some of the maps used in the article and S. Ryan for correcting the language.

References

Alcocer, J. A. E., M. V. García, H. S. Soto, D. Baltar, V. R. Paramo, P. Gabrielsen, and F. Roth, 2013, Reducing uncertainty by integrating 3D CSEM in the Mexican deep-water exploration workflow: First Break, **31**, 75–70.

Alcocer, J. A. E., M. V. García, H. S. Soto, F. Roth, D. Baltar, P. Gabrielsen, and V. R. Paramo, 2012, Experience from using 3D CSEM in the Mexican deepwater exploration program: 82nd Annual International Meeting, SEG, Expanded Abstracts, doi: 10.1190/segam2012-1181.1.

Baltar, D., and F. Roth, 2013, Reserves estimation methods for prospect evaluation with 3D CSEM data: First Break, **31**, 103–110.

Carstens, H., 2009, Striving to define an oil province: GeoExpro, **6**, no. 1.

Constable, S., 2010, Ten years of marine CSEM for hydrocarbon exploration: Geophysics, **75**, no. 5, 75A67–75A81, doi: 10.1190/1.3483451.

Darnet, M., M. C. K. Choo, R. Plessix, M. L. Rosenquist, K. Yip-Cheong, E. Sims, and J. W. K. Voon, 2007, Detecting hydrocarbon reservoirs from CSEM data in complex settings: Application to deepwater Sabah, Malaysia: Geophysics, **72**, no. 2, WA97–WA103, doi: 10.1190/1.2435201.

Eidesmo, T., S. Ellingsrud, L. M. MacGregor, S. Constable, M. C. Sinha, S. Johansen, F. N. Kong, and H. Westerdahl, 2002, Sea Bed Logging (SBL) a new method for remote and direct identification of hydrocarbon filled layers in deepwater areas: First Break, **20**, 144–152.

Ellingsrud, S., T. Eidesmo, and S. Johansen, 2002, Remote sensing of hydrocarbon layers by seabed logging (SBL): Results from a cruise offshore Angola: The Leading Edge, **21**, 972–982, doi: 10.1190/1.1518433.

Ellis, M., and P. Newton, 2013, Investigating electrical anisotropy drivers and modelling: Presented at 2nd International Workshop on Rock Physics, National Oceanography Centre.

Fanavoll, S., S. Ellingsrud, P. T. Gabrielsen, R. Tharimela, and D. Ridyard, 2012, Exploration with the use of EM data in the Barents Sea: The potential and the challenges: First Break, **30**, 89–93.

Fanavoll, S., B. Kjølhamar, C. S. Serck, and P. Gabrielsen, 2013, Lower Snadd — A new play model in the northern Barents Sea?: Presented at 2nd International CSEM conference: CSEM in hydrocarbon exploration and exploitation, Geological Society of Norway.

Gabrielsen, P. T., 1994, Syn-rift stratigraphic geometries in blocks 7219/9 and 7220/7: M.S. thesis, University of Trondheim.

Gabrielsen, P. T., P. Abrahamson, M. Panzner, S. Fanavoll, and S. Ellingsrud, 2013, Exploring frontier areas using 2D seismic and 3D CSEM data, as exemplified by multiclient data over the Skrugard and Havis discoveries in the Barents Sea: First Break, **31**, 66–73.

Gerdes, K., J. Hurst, and R. Jeans, 1992, Seismostratigraphic study of a synrift megasequence, from the

Barents Sea, northern Norway, *in* R. M. Larsen, H. Brekke, B. T. Larsen, and E. Talleraas, eds., Structural and tectonic modelling and its application to petroleum geology: NPF Special Publication, vol. 1, 133–152.

Kjølhamar, B., 2012, Hoop Basin — An integrated approach to 3D exploration in the Barents Sea: Presented at the Petroleum Potential of the Southwestern Barents Sea, NGS Conference.

Lorentz, L., H. T. Pedersen, and M. P. Buonara, 2013, First results from a Brazilian mCSEM calibration campaign: Presented at 13th International Congress of the Brazilian Geophysical Society.

Løseth, L. O., T. Wiik, P. A. Olsen, A. Becht, and J. O. Hansen, 2013, CSEM exploration in the Barents Sea: Part I — Detecting Skrugard from CSEM: 75th Annual International Conference and Exhibition, EAGE, Extended Abstracts, doi: 10.3997/2214-4609.20130731.

Maaø, F. A., 2007, Fast finite-difference time-domain modelling for marine-subsurface electromagnetic problems: Geophysics, **72**, no. 2, A19–A23, doi: 10.1190/1.2434781.

Mittet, R., 2010, High-order finite-difference simulations of marine CSEM surveys using a correspondence principle for wave and diffusion fields: Geophysics, **75**, no. 1, F33–F50, doi: 10.1190/1.3278525.

Mittet, R., and T. Schaug-Pettersen, 2008, Shaping optimal transmitter waveforms for marine CSEM surveys: Geophysics, **73**, no. 3, F97–F104, doi: 10.1190/1.2898410.

Narongsirikul, S., N. H. Mondol, and J. Jahren, 2013, Acoustic, electric, and petrophysical properties of mechanically compacted sands of varying mineralogy — Simulating the effects of uplift on rock properties: Presented at the 2nd International Workshop on Rock Physics.

Nguyen, A. K., Ø. Kjøsnes, and J. O. Hansen, 2013, CSEM exploration in the Barents Sea: Part II — High resolution CSEM inversion: 75th Annual International Conference and Exhibition, EAGE, Extended Abstracts, doi: 10.3997/2214-4609.20130732.

Zach, J. J., A. K. Bjørke, T. Støren, and F. A. Maaø, 2008, 3D inversion of marine CSEM data using a fast finite-difference time domain forward code and approximate Hessian-based optimization: 78th Annual International Meeting, SEG, Expanded Abstracts, 614–618.

Stein Fanavoll started his career in the Norwegian Petroleum Directorate as a seismic interpreter. Following that, he joined Sintef Petroleum Research, and later worked as a consultant, involved in E&P related projects. In 2002, he joined EMGS as a senior geophysicist, where his main task has been interpretation of CSEM data and integration with other geophysical data. With more than 20 years of exploration and 11 years of EM experience, he has a sound background for the current position as exploration advisor, working with interpretation of EM data together with seismic and other geophysical and geologic data.

Pål T. Gabrielsen received an M.S. (1994) in petroleum geology and geophysics from the Norwegian University of Science and Technology. He joined CGG in Oslo in 1996 to focus on seismic data processing. In 1997, he was the leader for a CGG dedicated seismic processing center at BP in Stavanger. He joined EMGS in 2004 with different positions related to G&G assignments. In 2009–2010, he was one of the founders of Vestfonna Geophysical and also the leader of the petroleum educational company GeoLearning. The last three years he is acting as a principal geophysicist with EMGS with focus on interpretation of CSEM data.

Svein Ellingsrud received an M.S. (1986) and a Ph.D. (1990) in physics from the Norwegian University of Science and Technology. He joined Statoil in Trondheim in 1992 as a research scientist to focus on petrophysics, rock physics, geophysics, and electromagnetic techniques. He was the project leader for the internal Statoil project that later became the background for establishing EMGS. In 2002, he joined EMGS as one of its founders and became vice president for research and development. He had responsibility for the technology development within EMGS until mid 2008. After 1.5 years as an executive adviser to KMS Technologies Inc., he rejoined EMGS in late 2009. Currently, he is the technical director for EMGS's multiclient business unit.